NSG-368

# AN ELECTROHYDRODYNAMIC INDUCTION PUMP

By

James R. Melcher

Department of Electrical Engineering
Massachusetts Institute of Technology
Cambridge, Massachusetts

## Abstract



An electrohydrodynamic traveling-wave induction interaction is shown to pump slightly conducting liquids (electrical conductivities $10^{-5}$ to $10^{-15}$ $(\Omega\text{-m})^{-1}$ ) without electrical contact with the flow. A gradient in fluid conductivity perpendicular to the direction of flow is required. Here, this is provided by a liquid interface, which is exposed to a traveling potential wave imposed by means of a segmented electrode parallel to the interface. Induced charges relax through the liquid to form a traveling-wave of surface-charge on the interface which lags the wave of image surface-charges on the electrode. Hence, a time-average electrical surface-traction is produced tending to make the fluid move with the traveling-wave. Expressions for the fields, the time average electric traction and the fluid velocity (in plane flow) are derived and discussed. Experiments illustrate the validity of these equations, and tend to support the model used for the interfacial conduction process.

Author

# AN ELECTROHYDRODYNAMIC INDUCTION PUMP

By

James R. Melcher

Department of Electrical Engineering
Massachusetts Institute of Technology
Cambridge, Massachusetts

## I. Introduction

Electrohydrodynamic pumping of liquids and gases by means of ion drag effects has received considerable attention in the literature.[1,2] These effects, which can also be used to generate electrical power,[3,4] take advantage of the drag produced when a carrier of electrical charge is introduced into a highly insulating fluid. Devices incorporating ion-drag effects require that electrical contact be made with the working fluid to implement the transfer of charge. In this sense, they can be referred to as conduction type devices, in that they are analogous to conduction magnetohydrodynamic pumps and generators.[5]

Another class of magnetic field devices makes use of induced currents to produce an electromechanical interaction. These induction machines are the most common rotating device,[6] and have been widely studied as magnetohydrodynamic pumps and generators[7,8].

An electrohydrodynamic pump is described here which makes use of induced charges to produce the basic electromechanical interaction. Like its magnetic analogue, it has the advantage that no electrical contact with the moving fluid is required, with no foreign particles or carriers introduced into the fluid.

This study has basic, as well as practical, implication. Stuetzer[9] has shown the usefulness of using electromechanical effects to study ion-drag conduction processes. Induction pump-

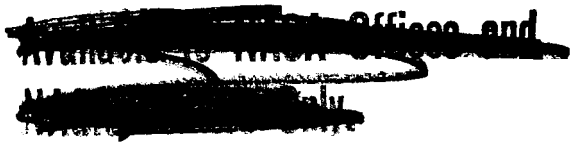

ing provides a means of studying natural conduction processes, in particular as they occur in the absence of electrode-liquid contacts, and as they are modeled at a free liquid-gas interface.

The induction pumping results when a wave of imposed potential travels in the direction of flow and perpendicular to a gradient in fluid conductivity. Here this gradient exists at the interface of a slightly conducting liquid and air, as shown in Fig. 1. For purposes of discussion, (and later experiments) the liquid is shown resting on a highly conducting plate, although this plate could just as well be insulating. The traveling potential wave is imposed by means of a segmented electrode parallel to the interface. Induced charges relax through the liquid to form a traveling-wave of surface charge on the interface, and this wave of charge lags the wave of image surface-charge on the electrode. Hence, a time-average electrical surface-traction is produced tending to make the fluid move with the traveling wave. Two points are essential: the bulk charge is zero (even though there are conduction currents within the volume of the fluid) and the net surface charge on the interface is zero. In the simple free-surface situation considered, all of the electromechanics occurs at the interface where there is a singularity in the gradient of the conductivity. There will be no interaction if the fluid is of uniform conductivity everywhere. These points will be discussed in Section II,, where the theoretical model is introduced. In Section II,, expressions for the fields, the time average electric traction and the fluid velocity are derived and discussed. In Section III, experiments illustrate the validity of these equations, and tend to support the model used for the interfacial conduction process.

## II. Theoretical Model

### Electric Fields and Charge Relaxation

The electric field $\bar{E}$ will be considered irrotational, since there are no large currents which would give rise to a significant magnetic induction. Hence,

$$\nabla \times \bar{E} = 0 \tag{1}$$

$$\nabla \cdot \varepsilon \bar{E} = q \tag{2}$$

where q is the free-charge density and $\varepsilon$ is the permittivity.

Conservation of free charge requires that

$$\nabla \cdot \bar{J} + \frac{\partial q}{\partial t} = 0 \tag{3}$$

The conduction process that gives rise to the free current $\bar{J}$ is most commonly represented by ohms law, which attributes a constant conductivity $\sigma$ to the material. Hence, in a frame moving with the fluid $\bar{J}' = \sigma \bar{E}'$. Galilean transformations for J' and E' to a fixed (unprimed) frame are $\bar{J}' = \bar{J} - q\bar{v}$ and $\bar{E}' = \bar{E}$ (implied by Eqs. (1), (2) and (3) ). It follows that the appropriate form of ohms law for the moving fluid is

$$\bar{J} = \sigma \bar{E} + q\bar{v} \tag{4}$$

This constitutive law implies that unless net free-charge is supplied to the fluid, the charge density q in the bulk of the fluid will decay. To see this, suppose that the fluid is incompressible. Then Eqs. (2), (3) and (4) combine to become

$$\frac{\partial q}{\partial t} + \frac{\sigma}{\varepsilon} q + \bar{v} \cdot \nabla q = 0 \tag{5}$$

This equation is satisfied if the charge density decays to $q = 0$. The effect of the velocity on the charge relaxation is apparent if plane flow is considered, as an example, so that $\bar{v} = v_x(y)$. Then, it follows from Eq. (5) that an initial charge density $q_o(x,y)$ will subsequently be given by

$$q = q_o\,[x - v_x(y)t, y]\,e^{-\frac{\sigma}{\varepsilon}t} \tag{6}$$

The convection redistributes the charge but does not alter the relaxation time $\varepsilon/\sigma$ for the decay of the charge density. Consideration is given here to sinusoidal steady-state phenomena, and so the charge density q in the bulk of the fluid is taken as zero.

Of course, there is a charge on the liquid interface and this fact is accounted for in the boundary conditions. These are,

$$\bar{n} \times (\bar{E}^u - \bar{E}^\ell) = 0 \tag{7}$$

$$\bar{n} \cdot (\varepsilon_o \bar{E}^u - \varepsilon \bar{E}^\ell) = Q \tag{8}$$

$$\sigma E_y^\ell = \frac{\partial Q}{\partial t} + \frac{\partial}{\partial x}(Qv_x) \tag{9}$$

on the interface at $y = 0$. The first and second of these conditions arise from the integration of Eqs. (1) and (2) across the interface, while the third results from an integration of Eqs. (3) and (4) across the interface. Here, Q is the surface charge density, and it has been assumed that fluid at the interface moves in the x direction and is bounded from above by a nonconducting gas. It is significant also that Eq. (9) does not include the possibility that an appreciable conduction of charge (due to a "surface conductivity") occurs within the interface. The only surface currents in this model arise from the convection of free surface charge.

Two additional boundary conditions on the electric field arise from the potential wave at y = d and the perfectly conducting plate at y = -a.

$$\frac{\partial E_x}{\partial x} = - \text{Re } \hat{V} \exp j(\omega t - kx); \; y = d \tag{10}$$

$$E_x = 0 \; ; \; y = -a \tag{11}$$

## Traveling-Wave Solutions

The electrical equations are linear, and hence it is reasonable to look for traveling electric field solutions by assuming that $\overline{E} = \text{Re } \bar{E}(y) \exp j(\omega t - kx)$. Then, Eqs. (1) and (2) have the solution,

$$\overline{E} = -\nabla \left[\text{Re } \hat{\Phi}(y) \exp j(\omega t - kx)\right] \tag{12}$$

$$\hat{\Phi} = - (A \cosh ky + B \sinh ky)/k$$

both above and below the liquid interface. To designate the solution above the interface, the constants A and B will be called $A_u$ and $B_u$. Similarly the constants below the interface are $A_\ell$ and $B_\ell$.

These four constants are determined by the four boundary conditions. Two of these arise because of the constraints placed on the potential at y = d (Eq. 10)

$$A_u \cosh kd + B_u \sinh kd = - k\hat{V} \tag{13}$$

and at y = -a (Eq. 11).

$$A_\ell \cosh ka - B_\ell \sinh ka = 0 \tag{14}$$

A third condition follows from Eq. (7)

$$A_u = A_\ell \tag{15}$$

while Eqs. (8) and (9) combine to give the last condition,

$$B_u - B_\ell \left( \frac{\varepsilon}{\varepsilon_o} - jS \right) = 0 \tag{16}$$

with $S = \sigma/\varepsilon_o \, (\omega - kU)$.

Here, U is the x component of the fluid velocity taken as constant in time and evaluated at the interface. The electric fields both above and below the interface are now known as a function of the interface velocity U and the amplitude $\hat{V}$ of the imposed potential wave.

## The Electric Surface Shear

The electric force density in a dielectric liquid arises from free charges ($q\bar{E}$) and from polarization charges ($-\frac{1}{2} E^2 \nabla \varepsilon$).[10] It has already been concluded that the simple Ohm's law conduction model used here requires that the first of these only exists as a transient. So long as the permittivity does not vary within the liquid, it is clear that the polarization force density in the bulk is also zero. That is, there are no electrical forces in the bulk of the liquid. All of the electromechanical coupling occurs at the interface, where there are both free- and polarization-charges.

Motions of the liquid in the x direction result because there is a net shearing traction on the interface which can be computed by integrating the free charge and polarization force densities across the interface (where they are singular). This is most conveniently done by expressing the total electric force density as $\nabla\cdot\bar{\bar{T}}$ , where the stress tensor $T_{ij}$ is[11]

$$T_{ij} = \varepsilon E_i E_j - \frac{1}{2}\delta_{ij}\varepsilon E^2 \tag{17}$$

It follows that the net force per unit area in the x direction on a section of the interface is

$$T_x = (\varepsilon_o E_y^u - \varepsilon E_y^\ell)E_x^u \tag{18}$$

where the fields are evaluated just above and below the interface.

The surface force is the product of sinusoidally varying electric fields. Hence, it has two components; one constant and the other varying at twice the frequency $\omega$ of the imposed traveling wave. The effect of the pulsating part of the electric traction will be ignored, with interest confined to the effect of the time average shearing force. From Eq. (18), this is

$$< T_x > = \frac{1}{4}\left[\hat{E}_x^u(\varepsilon_o\hat{E}_y^{u*} - \varepsilon\hat{E}_y^{\ell*}) + \hat{E}_x^{u*}(\varepsilon_o\hat{E}_y^u - \varepsilon\hat{E}_y^\ell)\right] \tag{19}$$

where $^*$ indicates the complex conjugate. Because $\hat{E}_x(0) = -jA$ and $\hat{E}_y(0) = B$, the time average surface traction is

$$< T_x > = \frac{1}{2}\frac{k^2\,\hat{V}\,\hat{V}^*\,\tanh ka\,S}{(\tanh ka\cosh kd + \frac{\varepsilon}{\varepsilon_o}\sinh kd)^2 + (S\sinh kd)^2} \tag{20}$$

Several limiting cases serve to illustrate the physical nature of the relaxation process which is responsible for this shearing traction. Note that if the conductivity $\sigma$ is very large, so that charges can relax instantaneously from one point on the interface to another, there is no shear. In this limit the electric field is perpendicular to the interface and therefore exerts no force in the x direction. Similarly, if the conductivity is too small so that no charges relax to the interface, the shear is small. This illustrates that there can be no surface force on an interface that does not support free-charge. Finally, if the phase velocity $\omega/k$ of the traveling wave of electric field is equal to the velocity U of the fluid at the interface, there is no shear. Pumping will take place only if there is a slip between the traveling wave and the fluid. These are all characteristics of induction type electromechanical devices.

The simple mechanism responsible for the surface traction of Eq. (20) is apparent from plots of the traveling fields, as shown in Fig. 2. Here, the distribution of potential resulting from the imposed potential wave on the electrode, is shown in Fig. 2a at an instant in time. The fields travel to the right, with charges induced on the electrode surface leading surface charges of opposite polarity on the interface (interface charges lag because they require time to relax to the interface). The resulting lines of electric field intensity are sketched in Fig. 2b. Here the electric field is skewed so as to produce a net shearing traction on the interface.

The induction mechanism does not depend on there being a conducting plate at $y = -a$, as shown in Fig. 1. This is illustrated by the field plots of Fig. 2, where the limit of $ka \rightarrow \infty$ is shown to indicate how the lines of electric field intensity return to the

interface when the distance to the bottom is large compared to the wavelength $2\pi/k$. A similar effect is obtained if the bottom is insulating, with the shape of the potential distribution distorted by the condition that no current flow through the insulating bottom.

## Fluid Motions

The fluid motions computed here are based on the effect of the time average traction. It is assumed that the fluid cannot respond to components of the traction at twice the frequency of the imposed traveling potential wave. This is an extremely good approximation unless the electric field participates parametrically in the instability of the interface. In experiments of the type discussed in Sec. III, stability of the interface imposes an important limitation on the electric pressure that can be used for pumping. There is a threshold for instability in a d-c electric field[12,13] that represents an upper bound on the useful electric pressure at high frequencies[14]. At low frequencies parametric effects can make this limitation even more stringent,[15] and it is in this regard that the pulsating component of the electric traction becomes significant. An indication of these limitations will be given in the next section.

Because there are no electrical forces in the bulk of the fluid, the well known solutions for laminar flow can be used to describe the fluid motions. The time average electric traction simply plays the role of a boundary condition (that depends on the fluid velocity). As an example, the experiments of the next section will be conducted on a re-entrant channel, so that there will be no longitudinal gradient in the pressure. Then, assuming that the depth (a) is small compared to the z dimension of the apparatus, the velo-

city profile is a linear function of y and is given by

$$v_x = U(1 + \frac{y}{a}) \tag{21}$$

It follows that the viscous shear at the interface is

$$T_{xy} = \mu \frac{\partial v_x}{\partial y} = \frac{\mu U}{a} \tag{22}$$

where $\mu$ is the viscosity.

The balance of electric (time average) shear and mechanical shear at the interface requires that

$$U = \frac{1}{2} \frac{a\, k^2\, \hat{V}^* \hat{V}\, \varepsilon_o \tanh ka\, S}{\mu (\sinh kd)^2 \left[ (\tanh ka \coth kd + \frac{\varepsilon}{\varepsilon_o})^2 + S^2 \right]} \tag{23}$$

which for a given value of S can be regarded as the required expression for the fluid velocity U at the interface. The largest value of U occurs when

$$S = \tanh ka \coth kd + \frac{\varepsilon}{\varepsilon_o} \tag{24}$$

in which case Eq. (23) becomes,

$$U = \frac{a}{4\mu} \frac{k^2\, \hat{V}\, \hat{V}^*\, \varepsilon_o \tanh ka}{(\sinh kd)^2 (\tanh ka \coth kd + \frac{\varepsilon}{\varepsilon_o})} \tag{25}$$

That is, the maximum velocity U is independent of the conductivity and frequency. Once it is evaluated from this expression, the value of S follows from Eq. (24) and this in turn fixes the possible values of conductivity and frequency.

Note that theoretically, the fluid can be propelled by the traveling field at a velocity given by Eq. (25) even if the conductivity approaches zero. It is simply necessary to provide a traveling wave in a nearly enough synchronous condition with the moving fluid that the optimum value of S is maintained. In this limit the pump becomes analogous to other electromechanical devices referred to as "synchronous" machines. The closest magnetic analogue is a rotating machine with a perfectly conducting (perhaps superconducting)[16] rotor, which very nearly conserves a magnetic flux. Here, the surface charge is very nearly conserved, and as with other "synchronous" devices, unless the traveling wave frequency is adjusted as the fluid is set into motion, the time average traction with the fluid stationary is very small (Eq. 20). To accrue a significant free surface-charge, the fluid must be nearly synchronous with the traveling potential wave so as to experience a potential frequency which is on the order of a reciprocal relaxation time.

## III. An Experimental Pump

### The Apparatus

An experiment to demonstrate the physical phenomena of electrohydrodynamic induction pumping is shown in Fig. 3. The fluid is contained within a re-entrant channel having insulating walls and a conducting bottom. Segmented electrodes are then positioned just above the free surface of the liquid as shown. The segments are connected individually to segments of a commutator ring, with interconnected divider resistors. The constant potentials $\pm V_o$ are then connected to graphite commutator contacts through slip rings. These contacts are mounted on a bar which rotates with the angular frequency $\omega$. At a given angular position, the divider resistors provide a potential distribution on the segments which varies linearly from a peak positive amplitude $V_o$ to a peak negative amplitude $-V_o$ (half way around the channel) and back to the potential $V_o$. Rotation of the commutator bar gives a traveling potential wave. This rather complicated means of obtaining a traveling wave was used to make a wave frequency that could be varied from zero to about six cps, while using a relatively simple electrode structure involving equi-area segments. More practical fully electrical schemes for making the traveling wave will be discussed.

The voltage waveform, taken from one of the segments, is shown in Fig. 4. The commutator switching is responsible for the high-frequency ripples in the voltage. In the experiments which follow, only the component of this wave form at the fundamental frequency is significant. This component is found (by numerical integration) to have an amplitude $0.66V_o$, where $V_o$ is the peak voltage of the "almost triangular" wave, shown in Fig. 4.

The mean circumference of the channel L was 0.886 m., with the electrode composed of 40 segments having the width of the channel (5.1 cm.) in the x (azimuthal) direction. The fluid (Monsanto Aroclor 1232, $\varepsilon = 5.7$ and $\sigma \cong 10^{-9}$ $(\Omega\text{-m})^{-1}$ ranged in depth from 0.5 to 4 cm and the electrode interface spacing d varied from 0.5 to 2 cm.

## Frequency and Voltage Dependence

Experiments were conducted to compare the dependence of the fluid velocity U as given by Eq. (23) on the applied potential $V_o$ and the frequency $\omega$. Under the optimum conditions represented by Eq. (24) the traveling wave of potential had a much larger velocity than that of the fluid, and hence, $S = \sigma/\omega\,\varepsilon_o$. Then, Eq. (23) not only shows that, at a given frequency, U should be proportional to the square of the peak potential $V_o$, but that at a given potential, U should have the frequency dependence

$$U = \frac{Af}{B + f^2} \tag{26}$$

where A and B are constants.

The measured dependence on $V_o$ of the fluid velocity U is shown in Fig. 5, where the solid line is the quadratic function of $V_o$ predicted by Eq. (23). The theoretical curve has been scaled to pass through the 8 kv. data points. A discussion of theory and experiment in predicting the absolute flow velocity is in the next section.

The experimental velocity U is shown as a function of frequency in Fig. 6. Here, the solid line has the frequency dependence of Eq. (26), again normalized to fit the data. This data clearly demon-

strates the optimum traveling wave condition given by Eq. (24). The velocities U in both Figs. 5 and 6 were measured by observing grains of plastic (having a density slightly less than that of the liquid) floating in the interface.

The conduction process in slightly conducting liquids is often dependent on the experimental history of the fluid. In the first hour of pumping under conditions of constant frequency and applied voltage, measurements of the type shown in Figs. 5 and 6 were found to drift. However, after about 2 hours, it was found that the experiments were reproducible. As an example, in Fig. 5, the multiple data points (at a given $V_o$) were taken in consecutive runs up and down the curve (over a period of two hours), with no trend observed in the data taken at a given voltage.

The upper limit in voltage, shown in Fig. 5, is imposed by the stability of the interface. At lower frequencies than about 2 cps, this limitation is more stringent because the sinusoidally varying electric traction leads to a parametric instability of the interface. In this case, small oscillations on the fluid interface are "pumped up" in synchronism with the surface traction, until the liquid interface begins to make contact with the electrode. At higher frequencies than about 2 cps, the impending instability appeared very much as observed in other experiments using d-c applied voltages,[17] with the interface deflection increasing monitonically with time until spikes were formed on the interface.

## Optimum Velocity

A quantitative comparison of the predicted and experimental magnitude of the optimum velocity was carried out using a thin layer of fluid (a = 0.75 cm ). This thin layer was used to make the aspect ratio (channel width/a) as large as possible in accordance with the assumptions for the fluid flow.

In the theory of Sec. II, it is implied that the electrode interface spacing is large enough compared to the x dimension of the segments (16 mm) to make the imposed potential at the interface appear essentially sinusoidal in space. Fig. 7 shows the measured dependence of the optimum velocity U on the electrode-interface spacing d with the electric field $V_o/d$ held constant. Under these conditions the theoretically predicted optimum velocity also has a dependence on d, as can be seen by taking the (appropriate) limit of Eq. (25) where $kd << 1$ and $ka << 1$. Then,

$$U = \frac{a^2 \varepsilon_o k (V/d)^2}{4\mu \left( \frac{a}{d} + \frac{\varepsilon}{\varepsilon_o} \right)} \qquad (27)$$

The theoretical curve in Fig. 7 is predicted by Eq. (27) with $V = 0.66V_o$ and $V_o/d = 10^6$ v/m. As would be expected, the agreement of theory and experiment improves as the spacing (d) becomes on the order of the segment dimension of 16 mm. Here, the fluid viscosity was $1.7 \times 10^{-2}$ N-sec/m$^2$. The accuracy of the theory in predicting the experimental velocity U at d = 16 mm is better than would be expected from the experimental control over such parameters as the voltage $V_o$, the spacing d and the viscosity, and it appears that the data are approaching a somewhat higher asymptotic value than indicated by theory. At larger spacings, fringing of the electrode

fields becomes significant. In any case, electrical break-down in the traveling-wave mechanism limited the range of d that could be investigated at this electric field.

At a spacing of 16 mm, the frequency which gave the largest velocity was 3.4 cps, and from Eq. (24) it follows that the fluid conductivity was about $1.2 \times 10^{-9} [\Omega\text{-m}]^{-1}$. This is about twice the apparent conductivity of a new sample of fluid measured using a conductivity cell under essentially the conditions used in the pump.

## IV. Conclusions and Observations

It is clear that the simple theory of induction pumping presented here is highly successful in predicting the dynamics of at least the one fluid used in the experiments. It appears from the theory that the electromechanical mechanism that has been demonstrated can be used with a wide range of liquids. In the limit where the conductivity is very small, the liquid can be pumped synchronously, with the practical limitation that the fluid be set into motion in synchronism with the traveling potential wave. To establish a sinusoidal distribution of static surface charge before the potential wave begins to travel would require about an hour with $\sigma \approx 10^{-15} (\Omega\text{-m})^{-1}$. This value of the conductivity seems to be a practical lower bound. The pumping of fluids having a conductivity greater than that used here also appears feasible. In this extreme, short relaxation times require that high frequency traveling waves be used. As the frequency is raised, magnetic induction effects eventually become important, and the electrohydrodynamic model introduced with Eq. (1) becomes invalid. An estimate of the highest conductivity of a liquid that can be motivated electrohydrodynamically is obtained by requiring that (for

example) a device one meter long be 1/10' of an (electromagnetic) wavelength at the frequency of the potential wave. That is, a 30 Mc/sec traveling wave can be used in such a device with no appreciable effect from magnetic induction. Then, for the electric induction interaction, $\omega\varepsilon/\sigma \gtrsim 1$, and it follows that fluids having a conductivity less than about $10^{-5}$ $(\Omega\text{-m})^{-1}$ can be induction pumped using the electrohydrodynamic scheme described here. Of course, it is possible to use a hybred magnetic and electric induction, and use still larger conductivities.

The pumping mechanism does not require that there be a free surface. For example, a transverse gradient in conductivity could be produced in a closed insulating conduit by cooling one of the walls. In this case, free charges would be induced by the traveling potential wave in the bulk of the liquid. This interaction is now under investigation.

For flexibility, a mechanical commutator was used here to make a traveling potential wave. In practice, two or three phase generators could be used to make a traveling wave by superimposing out-of-phase standing waves. Of course, this would necessitate using electrode segments of varying widths. However, the only mechanical motion in the resulting device would be that due to the fluid.

An attractive application of the induction process is not only to the pumping of liquids, but also to the measurement of fluid flow. Here, the fact that the induction process requires no electrical contact with the fluid is also a distinct advantage. Work concerned with electrohydrodynamic induction flow-meters will be reported.

Acknowledgments

The construction and testing of the experimental apparatus was carried out by Mr. E. Paul Warren, with the help of Lt. Millard Firebaugh. This work was supported by the National Aeronautics and Space Administration under NASA Research Grant NsG-368.

## References


1. O. M. Steutzer, J. Appl. Phys., 31, 136 (1960).
2. C. A. Timko, G. W. Penney and J. F. Osterle, Proc. IEEE, 53, 141, (1965).
3. R. E. Vollrath, Phys. Rev. 42, 298 (1932).
4. A. Marks, E. Barreto, and C.K. Chu, AIAA J. 2, 45 (1964).
5. G. W. Sutton and A. Sherman, Engineering Magnetohydrodynamics (McGraw-Hill Book Co., New York, 1965) p. 471.
6. D. C. White and H. H. Woodson, Electromechanical Energy Conversion (Wiley Book Co., Inc. New York, 1959) p. 238.
7. Penhune, J. P., "Energy Conversion in Laminar Magnetohydrodynamic Channel Flow", Ph.D. Thesis, Dept. Electrical Engineering M.I.T. (1961).
8. L. R. Blake, Proc. IEEE 104A, 49 (1957).
9. O. M. Stuetzer, Phys. of Fluids, 6, 190 (1963).
10. J. A. Stratton, Electromagnetic Theory, (McGraw-Hill Book Co. Inc., 1941) p. 145.
11. ibed, p. 147.
12. J. R. Melcher, Field-Coupled Surface Waves, (M.I.T. Press, Cambridge, Massachusetts, 1963) p. 61.
13. G. I. Taylor and A. D. McEwan, J. Fluid Mech., 22, 1 (1965).
14. E. B. Devitt and J. R. Melcher, Phys. of Fluids, 8, 1193, (1965).
15. J. M. Reynolds, Phys. Fluids 8, 161 (1965).

## References (cont.)

16. Z. J. J. Stekly and H. H. Woodson, IEEE Trans. on Aeorspace, AS-2, 826 (1964).

17. J. R. Melcher, op. cit., p. 65.

## Figure Captions

Figure 1. Cross-sectional view of pump, showing a slightly conducting liquid of depth (a) resting on a rigid conducting plate. The interface (at y = 0) is exposed to a traveling potential wave imposed by a segmented electrode at y = d. A traveling wave of surface charge is induced on the interface.

Figure 2. Cross-sectional view of the segmented electrode with the imposed potential wave $v = \mathrm{Re}\ \hat{V} \exp j(\omega t - kx)$. For these sketches it is assumed that $\varepsilon/\varepsilon_o = 1$, $S = 1$, $kd = 0.5$ and $ka \rightarrow \infty$. a) Equipotential lines and net surface charges induced on the electrode and on the liquid surface. Note that charges on the interface lag their images on the electrode. b) Lines of electric field intensity, showing a net surface traction in the x direction.

Figure 3. The experimental apparatus, showing both the pump and the mechanism for making the traveling potential wave. The slightly conducting liquid is contained in a channel having insulating walls and a conducting bottom. Segmented electrodes just above the interface are connected to d-c voltage sources through divider resistors so that there is a "saw-tooth" distribution of potential around the channel. This distribution is made to travel by rotating the commutator bar at the frequency $\omega$.

Figure 4. The voltage, as a function of time, recorded on one of the segments shown in Fig. 3. High-frequency components of the wave-form are due to commutator sparking. The fundamental component is $0.66V_o$, where $V_o$ is the peak voltage.

Figure 5. The liquid velocity U (at the channel center) as a function of the peak electrode potential $V_o$. The solid curve has the theoretical quadratic dependence on $V_o$ and is normalized to the 8 kv data point. The data was taken up and down the curve over a

period of two hours after the liquid had been "aged" for about two hours. (The fluid was Monsanto Aryclor -1232, with d = 1 cm., a = 3.5 cm. and f = 2 cps.).

Figure 6. Liquid velocity U as a function of the potential frequency f. Because the traveling wave velocity was considerably greater than U, the data should take the form of the solid line, as predicted by Eq. (26) normalized to pass through the peak velocity point. Experimental conditions are as in Fig. 5.

Figure 7. Absolute velocity U as a function of the electrode-interface spacing d, with $V_o/d$ held fixed. The solid line is theoretical. The data shows how the degrading effect of the finite segment size (16 mm) diminishes as the electrode-interface spacing increases.

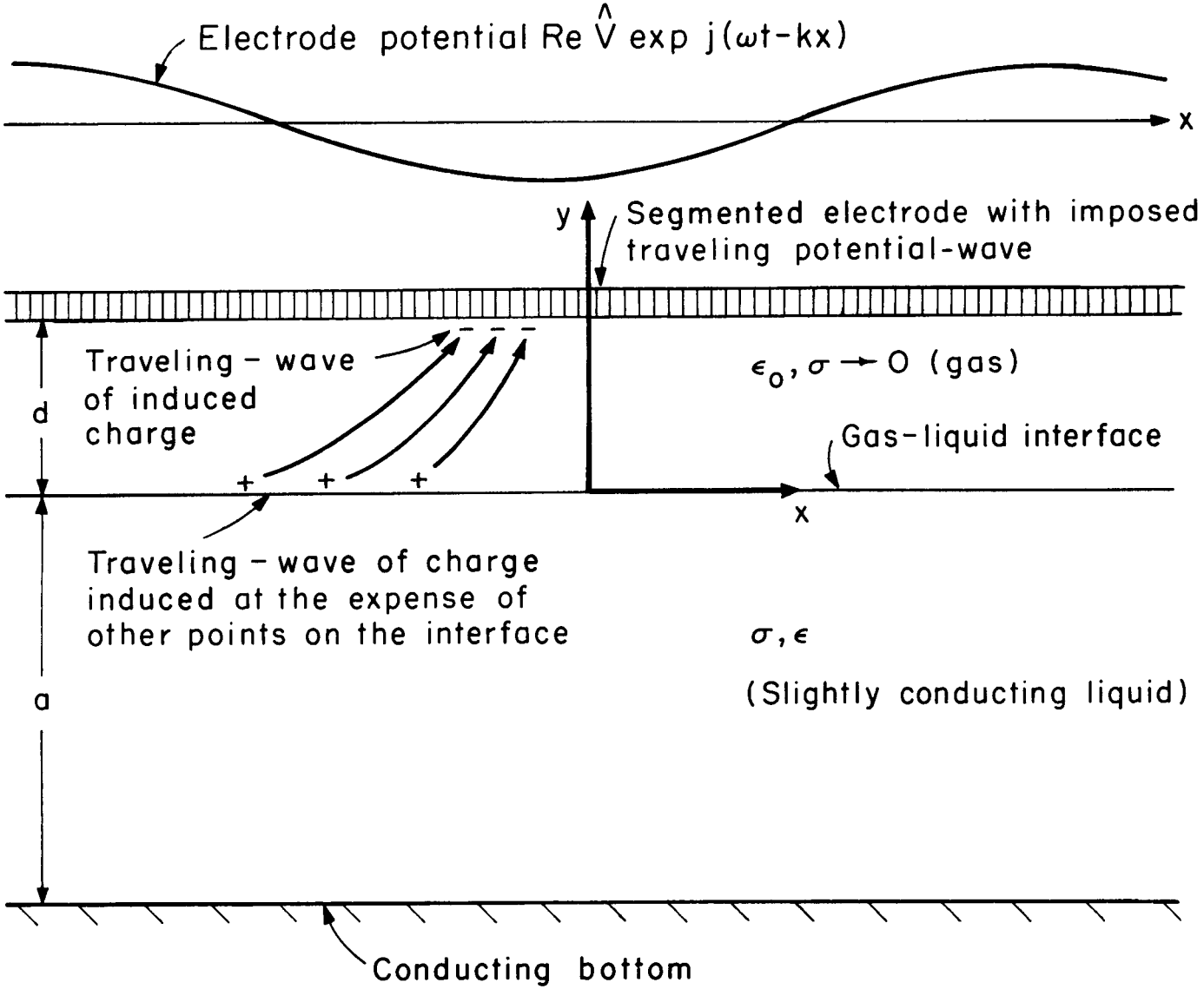


**Figure 1**. Cross-sectional view of pump, showing a slightly conducting liquid of depth (a) resting on a rigid conducting plate. The interface (at y = 0) is exposed to a traveling potential wave imposed by a segmented electrode at y = d. A traveling wave of surface charge is induced on the interface.

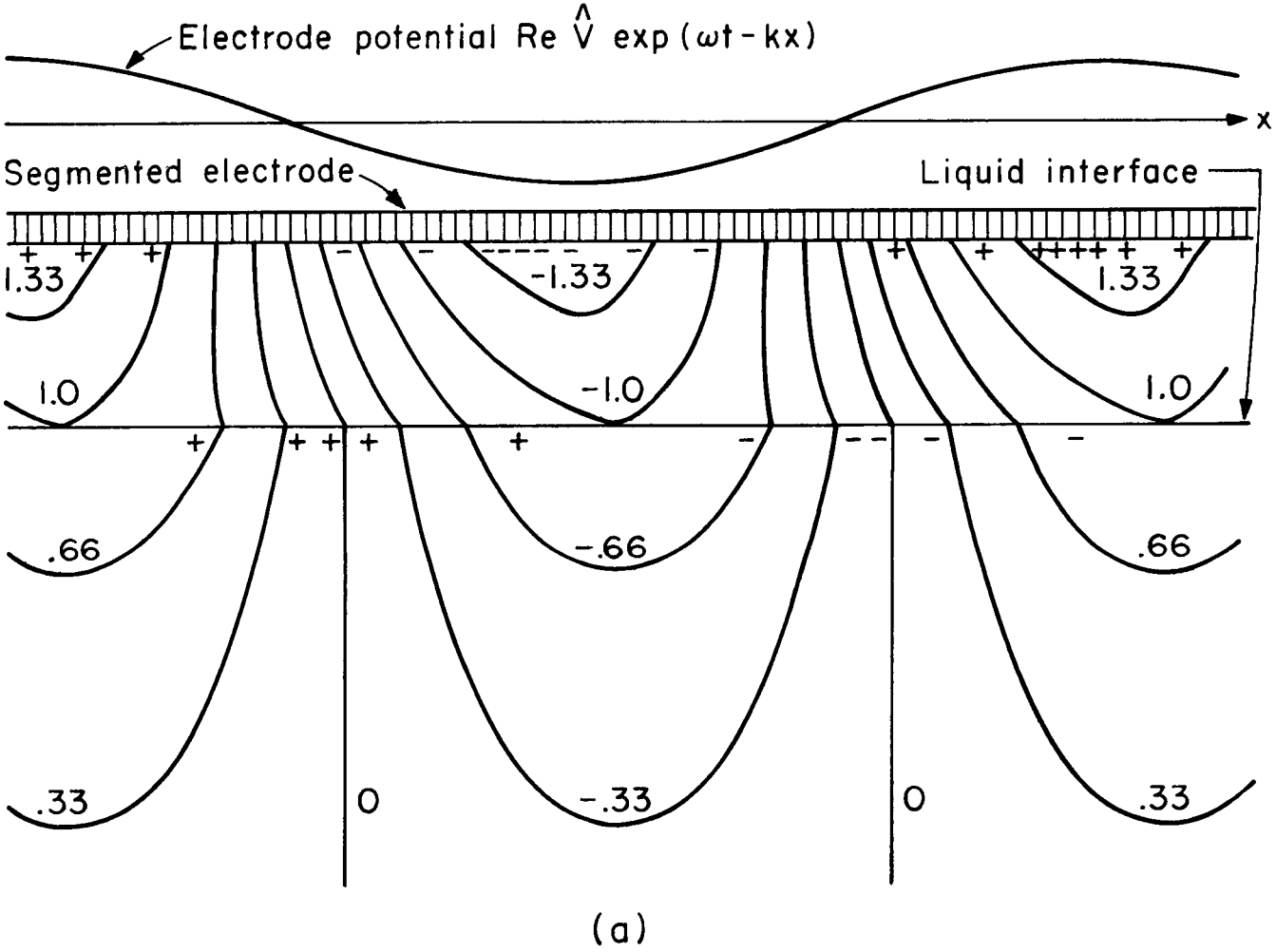


Figure 2. Cross-sectional view of the segmented electrode with the imposed potential wave v = Re $\hat{V}$ exp j (ωt-kx). For these sketches it is assumed that $\varepsilon/\varepsilon_o$ = 1, S = 1, kd = 0.5 and ka $\rightarrow \infty$ . a) Equipotential lines and net surface charges induced on the electrode and on the liquid surface. Note that charges on the interface lag their images on the electrode. b) Lines of electric field intensity, showing a net surface traction in the x direction.

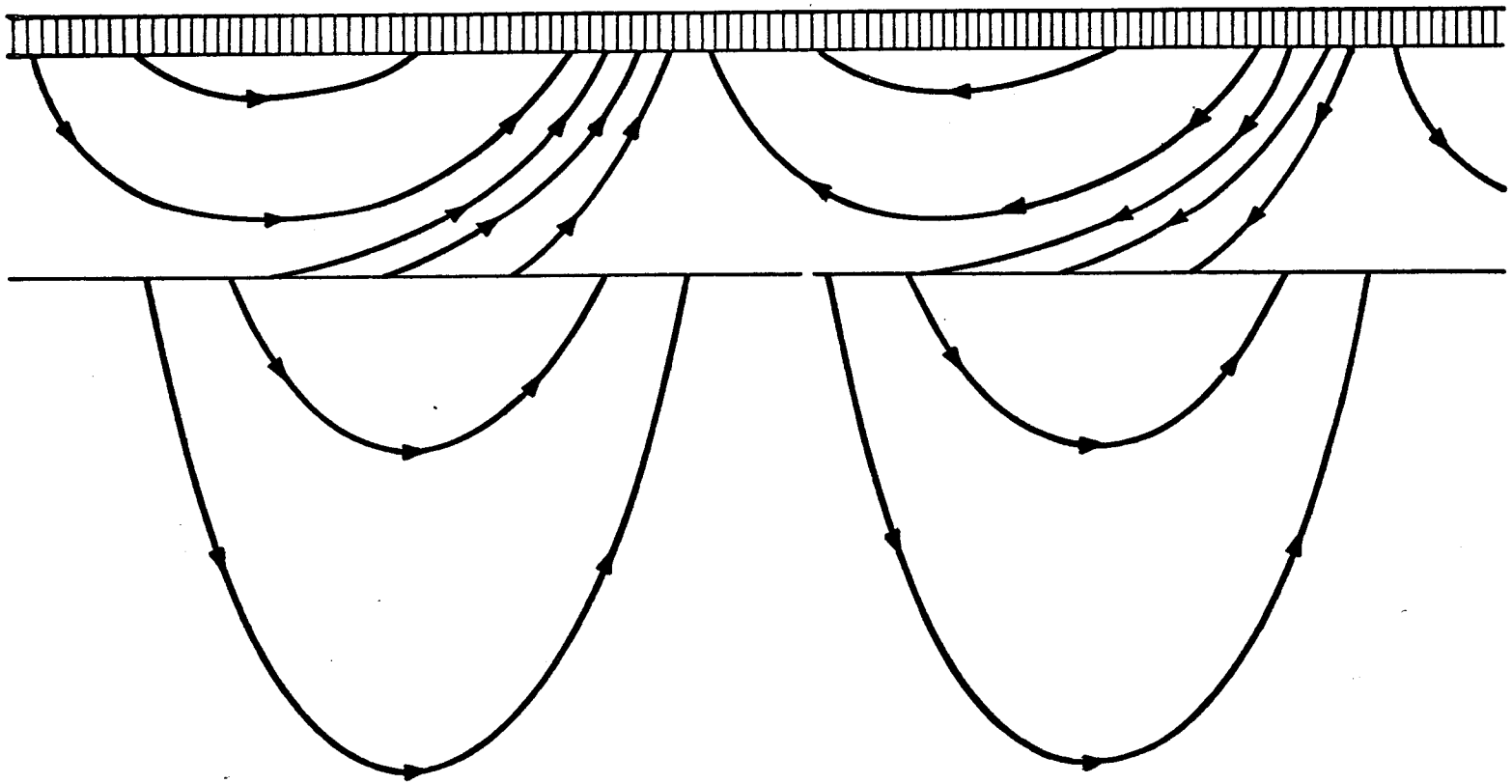

(b)

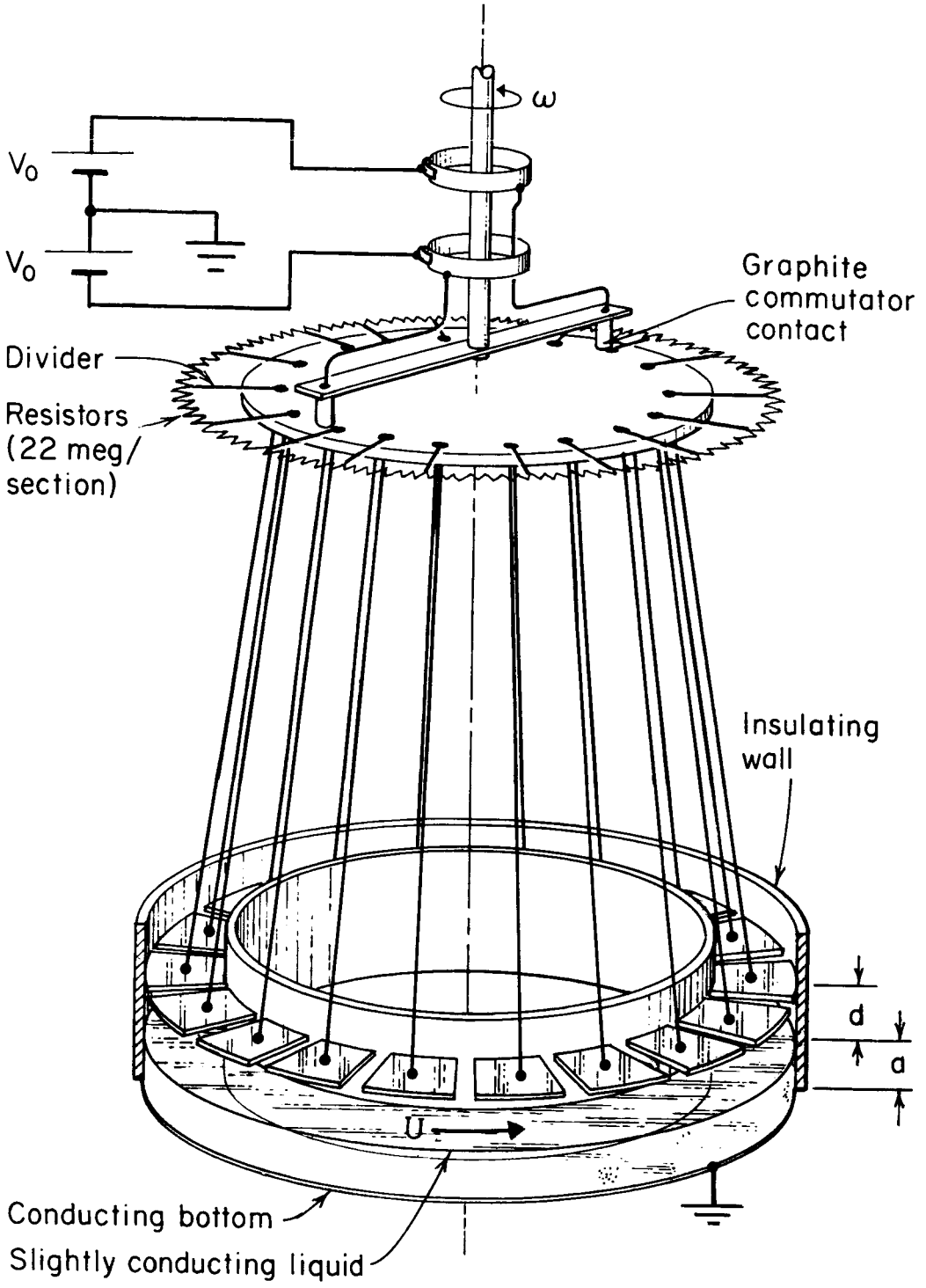


Figure 3. The experimental apparatus, showing both the pump and the mechanism for making the traveling potential wave. The slightly conducting liquid is contained in a channel having insulating walls and a conducting bottom. Segmented electrodes just above the interface are connected to d-c voltage sources through divider resistors so that there is a "saw-tooth" distribution of potential around the channel. This distribution is made to travel by rotating the commutator bar at the frequency $\omega$.

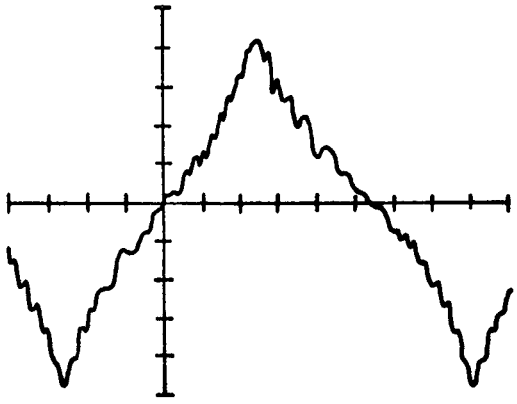

Figure 4. The voltage, as a function of time, recorded on one of the segments shown in Fig. 3. High-frequency components of the wave-form are due to commutator sparking. The fundamental component is $0.66V_o$, where $V_o$ is the peak voltage.

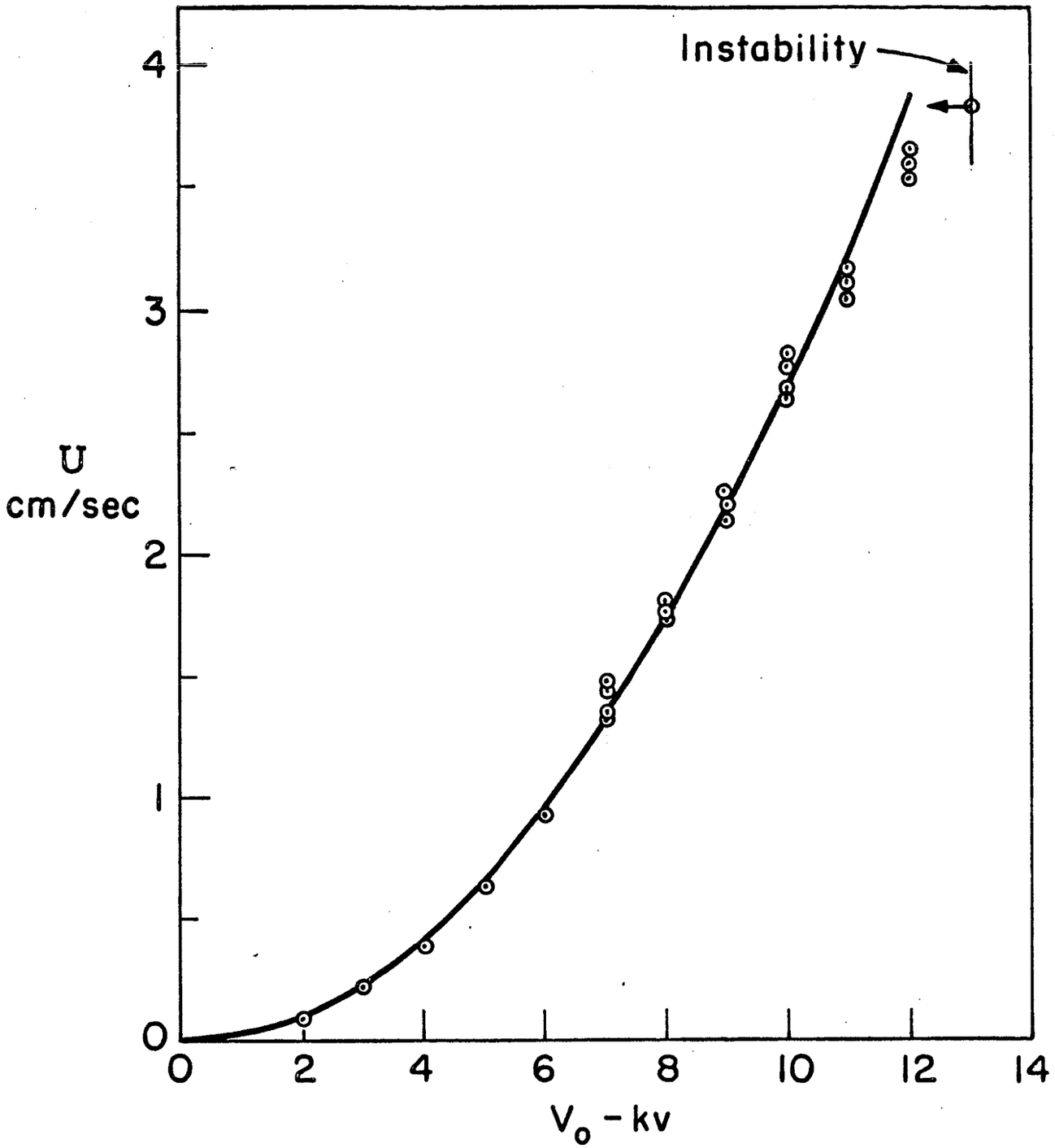


Figure 5. The liquid velocity U (at the channel center) as a function of the peak electrode potential $V_o$. The solid curve has the theoretical quadratic dependence on $V_o$ and is normalized to the 8 kv data point. The data was taken up and down the curve over a period of two hours after the liquid had been "aged" for about two hours. (The fluid was Monsanto Aryclor -1232, with d = 1 cm , a = 3.5 cm and f = 2 cps.).

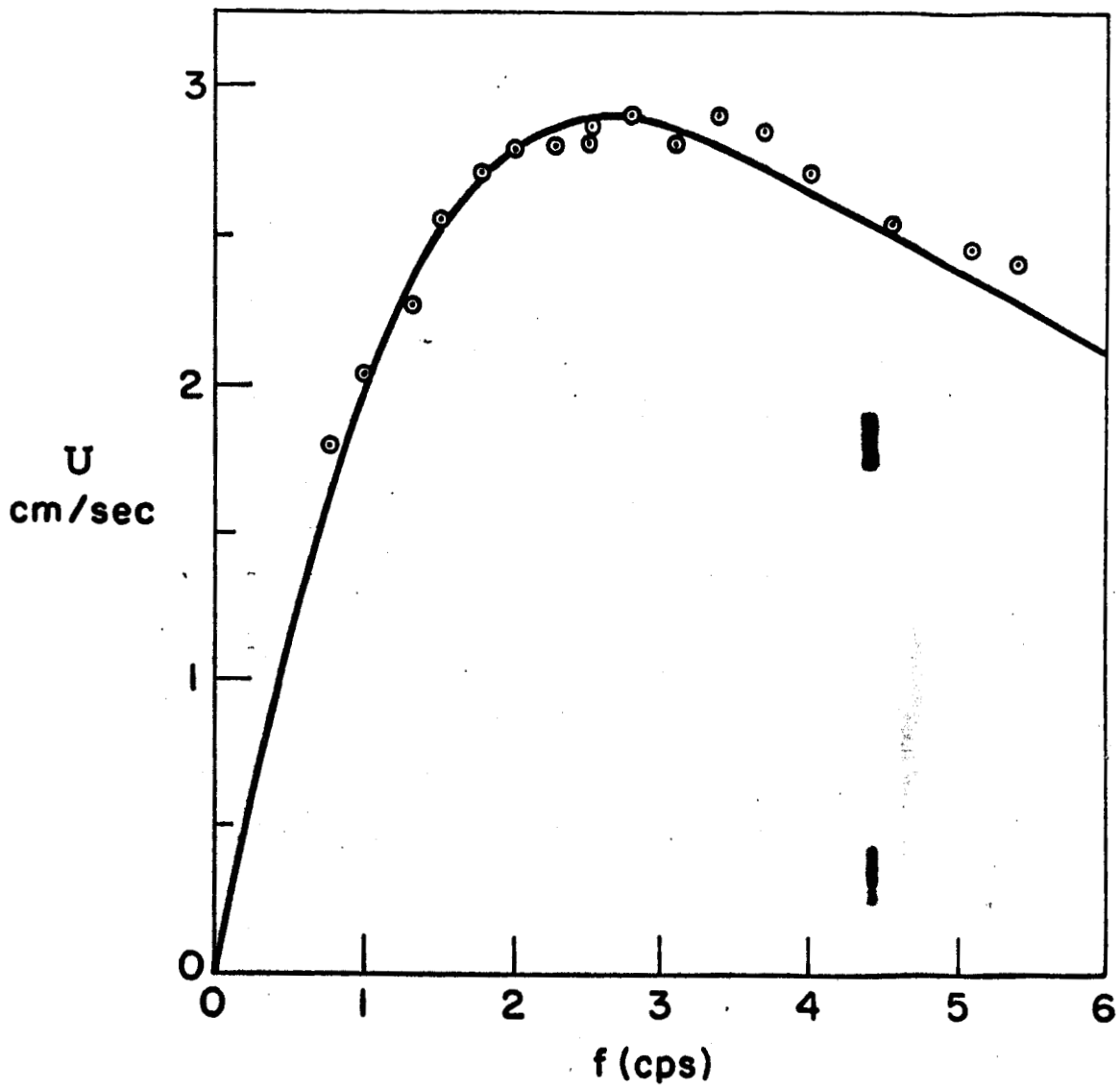


Figure 6. Liquid velocity U as a function of the potential frequency f. Because the traveling wave velocity was considerably greater than U, the data should take the form of the solid line, as predicted by Eq. (26) normalized to pass through the peak velocity point. Experimental conditions are as in Fig. 5.

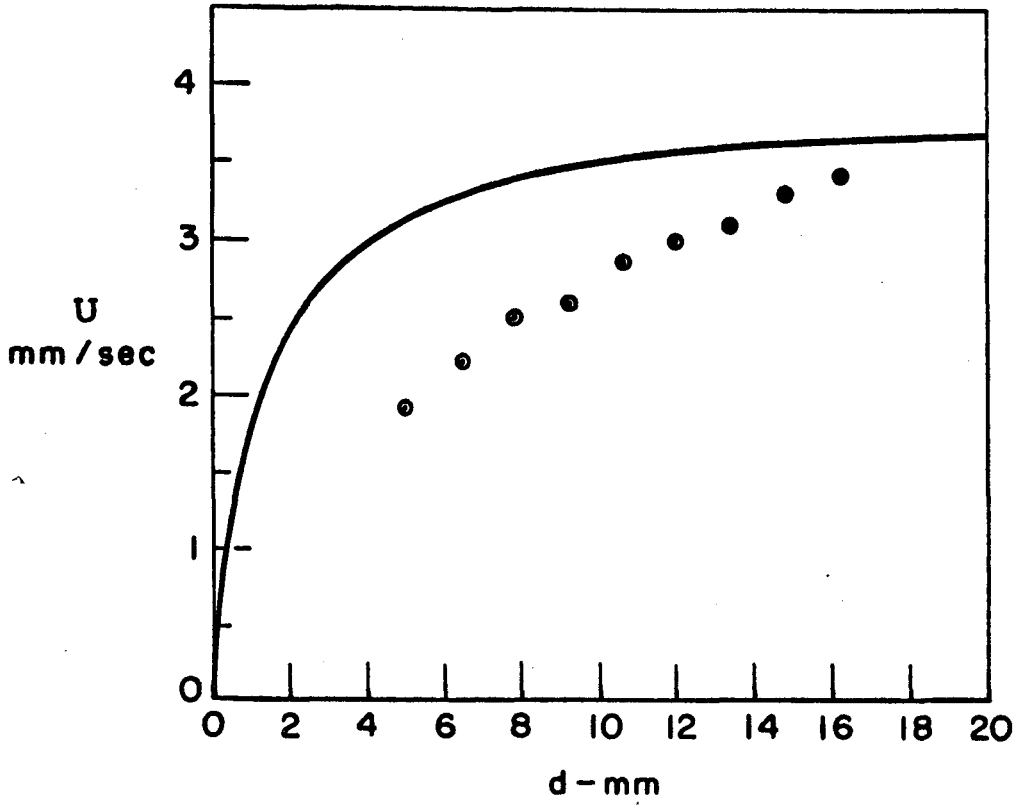


Figure 7. Absolute velocity U as a function of the electrode-interface spacing d, with $V_o/d$ held fixed. The solid line is theoretical. The data shows how the degrading effect of the finite segment size (16 mm) diminishes as the electrode-interface spacing increases.